

L.DIETRICH, W.SZCZEPIŃSKI

Plastic Yielding  
of Axially-Symmetric Bars  
with Non-symmetric V-notch

5/1967

WARSZAWA 1967



Do użytku wewnętrznego

---

Zakład Mechaniki Ośrodków Ciągłych IPPT PAN  
Nakład 150 egz. Ark.wyd.0,9. Ark.druk.1,25.  
Druk ukończono w lipcu 1967 r.

---

Warszawska Drukarnia Naukowa  
Warszawa, ul.Sniadeckich 8

Zam. 595/0/67.

PLASTIC YIELDING OF AXIALLY-SYMMETRIC BARS WITH NON-SYMMETRIC  
V-NOTCH

L.DIETRICH and W.SZCZEPINSKI, WARSAW

I. Introduction

The problem of the stress distribution and mode of deformation of plane strain and plane stress notched bars of a perfectly plastic-rigid material is rather well elaborated. A number of papers dealing with this problem have been published starting from the classic papers by Hill [1] and Bishop [2]. For axially symmetric notched bars, however, the solution based on the Huber-von Mises yield criterion and the associated flow rule is still unavailable, because as shown by Hill [3] the system of equations is not hyperbolic and therefore the method of characteristics cannot be used.

Shield [4] has shown that if the Tresca yield criterion with the associated flow rule, along with the Haar-Karman hypothesis, is employed, the system of governing equations becomes hyperbolic. He presented the numerical solution to the problem of indentation of a plastic infinite body by a flat axially symmetric punch. As shown by McClintock [5] this solution may be applied to the problem of an axially symmetric bar with a slit-shaped notch undergoing tension. This can be done by simply changing respectively signs and indexes of stresses and velocities.

Analogous solution for bars with V-shaped and various rounded notches, along with the experimental verification, have been presented in the previous paper [6].

In this study section 3 the plastic incipient flow of V-notched axially symmetric bars with different slope of both generators is considered. The theoretical solution shows that the yield point load is then greater than for a symmetrically notched bar. This effect is similar to that obtained for the punch indentation problem [7] under conditions of axial symmetry where, in contrast to the analogous plane strain solution, the yield point average stresses over the surface of the punch are greater for the rough punch than for a smooth one.

Theoretical yield point loads have been verified experimentally. Three sets of notched specimens of an aluminium alloy have been tested. The experimental results demonstrate that the yield point load calculated for perfectly plastic material has real significance for ductile metals.

## II. Basic equations.

The detailed analysis of the axially symmetric flow of a rigid-plastic material obeying the Tresca yield criterion and the associated flow rule is given by Shield [4]. To make this paper sufficiently self-contained a number of necessary equations will be given below.

The stresses at any point of the plastic region of the axially symmetric notched bar are represented in the principal stress space  $\bar{\sigma}_1, \bar{\sigma}_2, \bar{\sigma}_3$  by points located on that edge of the Tresca hexagonal prism for which

$$\bar{\sigma}_2 = \bar{\sigma}_3, \quad (1)$$

and

$$\bar{\sigma}_1 - \bar{\sigma}_2 = 2k, \quad (2)$$

where  $\sigma_1$  and  $\sigma_2$  ( $\sigma_1 > \sigma_2$ ) are the principal stresses in the meridional plane, and  $\sigma_3 = \sigma_\theta$  is the circumferential stress.

Since equations (1) and (2) impose two independent conditions on the four stress components  $\sigma_r$ ,  $\sigma_z$ ,  $\tau_{zr}$  and  $\sigma_\theta$  the state of stress may be expressed by two independent parameters  $\psi$  and  $p$ , whose meaning is indicated in fig.1. Consequently we can write

$$\begin{aligned} \sigma_z &= p + k \sin 2\psi, & \tau_{zr} &= k \cos 2\psi, \\ \sigma_r &= p - k \sin 2\psi, & \sigma_\theta &= p - k. \end{aligned} \quad (3)$$

The substitution of the expression into the equilibrium equations yields a hyperbolic system of two quasi-linear partial differential equations with two unknown functions  $p$ ,  $\psi$  and two independent variables  $r$ ,  $z$ . The equations of the characteristics of this system have the form

$$\frac{dz}{dr} = \tan \psi, \quad dp - 2k d\psi = \frac{k}{r}(dz - dr) \quad (4a)$$

for the first family of lines, called later  $\alpha$ -family, and

$$\frac{dz}{dr} = -\cot \psi, \quad dp + 2k d\psi = -\frac{k}{r}(dz + dr) \quad (4b)$$

for the second family, called  $\beta$ -family.

The vector of the flow velocity in the meridional plane  $r$ ,  $z$  can be expressed by the components  $v_\alpha$  and  $v_\beta$  along the  $\alpha$  and  $\beta$  lines, respectively. If use is made of the isotropy condition and of the incompressibility condition, these components must satisfy the equations

$$\begin{aligned} dv_\alpha - v_\beta d\psi &= - (v_\alpha \cot \psi - v_\beta) dz/2r && \text{along an } \alpha\text{-line,} \\ dv_\beta + v_\alpha d\psi &= (v_\alpha \cot \psi - v_\beta) dr/2r && \text{along a } \beta\text{-line.} \end{aligned} \quad (5)$$

Equations (5) were given by Hill [3] and later by Shield [4].

For the velocity field to be associated with the stress field the following inequalities must be satisfied

$$\dot{\epsilon}_1 \gg 0, \quad \dot{\epsilon}_2 \ll 0, \quad \dot{\epsilon}_3 < 0, \quad (6)$$

where  $\dot{\epsilon}_1$  and  $\dot{\epsilon}_2$  are the principal strain rates in the  $r, z$  plane, and  $\dot{\epsilon}_3 = \dot{\epsilon}_\theta$  is the circumferential strain rate.

The solution of particular problems consists in numerical or graphical integration of the equations (4) and (5). Solving subsequently appropriate boundary value problems for stresses and velocities, we finally obtain the stress and velocity fields. In this paper solutions are obtained by a graphical method elaborated by Mróz [9] for axially symmetric plastic flow.

### III. Stress fields

Let us consider a V-notched axially symmetric bar with different slope of both generators (Fig.2). The generator of the upper part of the notch makes with the  $r$ -axis the angle  $\omega$ , while the generator of the lower part makes the angle  $\tau$  being smaller than  $\omega$ . The bar is loaded by two opposite tensile forces. Graphical solutions were obtained for notches with angles  $\omega = 60^\circ$  (Fig.3) and  $\omega = 30^\circ$  (Fig.4).

The stress field in region  $AEC$  is determined by the stress free surface  $AB$ , the fan at the singular point  $A$  being terminated by the slip-line  $AC$  which meets the axis of symmetry at an angle of  $45^\circ$  at  $C$ .

The extensions of the stress field into the upper and lower rigid parts of the bar were obtained by assuming the material to be fully plastic.

The extension into the upper part is similar to that given by Eason and Shield [7] for the punch indentation problem. The  $\alpha$ -line  $EC$  together with the condition that slip-lines meet the axis of symmetry at angles  $45^\circ$ , determines the stress field to the left of the  $\beta$ -line through  $B$ . The field to the right of the  $\beta$ -line through  $B$  may be obtained by solving the inverse Cauchy boundary value pro-

blem, assuming the line EK to be hypothetical stress-free surface of the bar. Depending on the value of the angle  $\omega$  one or two shocks are introduced at the points M and N, where the  $\beta$ -lines begin to intersect one another. The discontinuity lines are shown by broken lines. The hypothetical stress-free boundary is parallel to the axis of symmetry at the point K. The stress-discontinuity line KE is terminating the stress field. Above KE the stress is uniaxial tension or compression parallel to the z-axis and not violating the yield criterion as shown in both figures.

Let us consider now the extension into the lower part of the bar. The  $\beta$ -line AC together with the condition that slip-lines meet the axis of symmetry at angles of  $45^\circ$  determines the stress field in the curvilinear triangle ACOH. The angle of the slip-line fan at A must be equal to the angle of the upper fan at A. The stress-free boundary AF was obtained in the same manner as the upper boundary ABK. Depending on the value of  $\omega$  the stress discontinuities are introduced at the point P or R, where the  $\alpha$ -lines begin to intersect one another. The stress field was terminated by the stress discontinuity line FG, below which the stress is uniaxial tension or compression. The calculated values of stresses shown in Figs. 3 and 4 do not exceed the yield point.

The total forces acting on both terminating discontinuity surfaces KE and FG were found to be within 6.3 % of the force calculated on the narrowest cross-section AC. This discrepancy may be attributed to the inaccuracy of the graphical method used in this work.

The stress fields obtained for both cases are statically admissible and the calculated yield point loads are lower bounds for the tensile force.

It is interesting to note that the smaller is  $\omega$  the more the tangent line to the stress-free surface AF at A approaches to the generator AB of the upper part of the notch. For  $\omega = 24^\circ$  we have  $\omega = \delta$  and both lines coincide. Thus the solution obtained for  $\omega = 24^\circ$  is valid for the limit case of the slit-notch making an angle of  $24^\circ$  with the r-axis as shown in Fig.5. If  $\omega < 24^\circ$  the solution of type described above cannot be constructed, because the stress-free boundary AF of the lower extension of the stress field intersects the boundary AB of the upper part of the bar.

The total load of the incipient plastic flow has been obtained for both calculated cases  $\omega = 60^\circ$  and  $\omega = 30^\circ$  by means of numerical integration along the radius OA of the narrowest cross-section

$$P^* = 2\pi \int_0^R \sigma_x r dr . \quad (7)$$

The yield point load factor of the notched bar will be defined as the ratio

$$f = P^*/P_0 , \quad (8)$$

where  $P_0 = 2\pi R^2 k$  is the yield point load of the smooth bar with the diameter  $2R$ .

For  $\omega = 60^\circ$  the yield point load factor is  $f_{60^\circ} = 1.75$  and for  $\omega = 30^\circ$  is found to be  $f_{30^\circ} = 2.42$ . For  $\omega = 90^\circ$  it is obviously  $f_{90^\circ} = 1.00$ . The continuous line 1 in Fig.6 plotted through the calculated points gives the value of the load factor for an arbitrary angle  $\omega$  of the notch. The lower continuous line 2 gives the load factors for symmetrically V-notched bars [6], i.e. for  $f = \omega$ . The exact values of the load factors for non-symmetrically notched bars with angles  $\omega < 24^\circ$  are not known. For practical purposes, however, their approximate values may be obtained from the straight line through the points A and B. The dashed line 3 shows the load



factor values for plane strain bars with V-shaped notches.

#### IV. Velocity field

Let us assume that the incipient plastic flow is confined to the region ABC. The rigid parts of the bar move with the velocity  $v_0$  as shown in Fig. 2. It is more convenient, however, to assume without loss of generality, that the upper part of the bar is fixed ( $v = 0$ ) and the lower part moves downwards with the velocity  $2v_0$ . Such conditions can be obtained by superposition of the rigid translation of the bar downwards with the velocity  $v_0$ .

The velocity field in the region ABC must satisfy the conditions that the normal velocity across  $\beta$ -line AC is continuous and that the normal velocity across  $\alpha$ -line BC is zero. Thus along BC  $v_\beta = 0$  and the first of equations (5) gives

$$v_\alpha = A/\sqrt{r} \quad \text{on BC,}$$

where A is a constant. To avoid an infinite value of  $v_\alpha$  at C the constant A must be set equal to zero. Thus

$$v_\alpha = v_\beta = 0 \quad \text{on BC,} \quad (9)$$

The condition that the normal velocity across AC must be continuous implies

$$v_\alpha = 2 v_0 \sin\psi \quad \text{on AC,} \quad (10)$$

Thus the second of equations (5) takes the form

$$dv_\beta + 2 v_0 \sin\psi d\psi + (v_\beta - 2 v_0 \cos\psi) \frac{dr}{2r} = 0. \quad (11)$$

Integrating this equation we obtain

$$v_\beta - 2 v_0 \cos\psi = \frac{B}{\sqrt{r}}, \quad (12)$$

where B is a constant. A similar argument to the above shows that  $B = 0$ , so that

$$v_\beta = 2 v_0 \cos\psi \quad \text{along AC.} \quad (13)$$

The conditions (9) and (13) constitute the characteristic boundary value problem for the velocity equations (5), and define the

velocity field in the entire region ABC. Since the velocity problem is similar to that considered by Eason and Shield [7], the same procedure may be used in our case. In the present study this field has not been calculated, and therefore the numerical check of inequalities (6) could not be made.

#### V. Experimental results

Three sets of specimens were tested to determine the yield point for axially symmetric bars with various angles  $\omega$ . The material of all specimens was the aluminium alloy PA3 (according to polish standards) containing 5 percent of magnesium.

A universal hydraulic testing machine and hinge-type fittings were used in order to minimize the possible bending of the bar. Deformations were recorded by means of a mechanical extensometer with two 0.01 mm division dial gauges and 60 mm gauge length, applied on the surface of each specimen at diametrically opposite positions. In order to eliminate possible slight deviations from symmetry, the deformations were taken as the mean value of readings of both dial gauges. It was found that such measuring technique assures good reproducibility of experimental results.

In the first set six specimens with various angles  $\omega$  have been tested. Dimensions of specimens are shown in Fig. 7, where also initial portions of the conventional stress  $\bar{\sigma} = P/F_0$  ( $F_0 = \pi R^2$ ) - elongation  $\Delta l$  diagram are presented. Since the diagrams do not display clearly visible yield point stresses, a conventional definition of the yield average stress  $\bar{\sigma}^*$  is introduced as the point at which the tangent modulus reaches the value  $0.3 \tan \alpha$ , where  $\alpha$  is the angle which makes the initial straight portion of the diagram with the elongation axis. The actual yield point load factor was then calculated from the formula  $f = \bar{\sigma}^*/\bar{\sigma}_0$ , where  $\bar{\sigma}_0$  is the actual average

yield point stress obtained experimentally for an unnotched bar. The experimental values of the load factor are shown as small stars in Fig.6.

In the same manner a set of specimens with symmetrical notched ( $\omega = \gamma$ ) has been tested. The material was also the PA3 aluminium alloy and the same measuring technique has been used. The experimental yield point load factors are marked in Fig.6 by small circles.

In the last set 13 specimens of the PA3 aluminium alloy were tested. All dimensions including notch angle were the same except the diameter  $2c$  of the upper part (Fig.8). Thus the influence of the  $c/R$  ratio on the yield point load has been investigated. Fig.8 shows some of the obtained conventional stress-elongation diagrams for various  $c/R$  ratios. Arrows indicate the conventional yield point average stress estimated in the manner described above. Thus obtained yield point stresses are shown by small circles in Fig.9.

The heavy lines show the theoretical estimates of yield point average stresses. For  $c/R > 1.78$  the extended slip-line field from Fig.3 lies entirely within the actual contour of the upper part of the bar. Thus to the right of  $c/R = 1.78$  the yield point stress is constant for arbitrary  $c/R$ . For  $c/R < 1.78$  the exact solution is still unavailable and the lower and upper bounds on the yield point load can only be calculated. A lower bound may be obtained from the field shown in Fig.10. If the actual  $c/R$  ratio is too small for the given  $\omega_1$ , we can always find such an angle  $\omega_2$  for which the extended stress field will be inscribed entirely within the actual contour of the bar. The load factor taken from Fig.6 for  $\omega_2$  furnishes a lower bound on the actual load factor. An upper bound on the yield point load may be found by equating the work done by both

tensile forces  $P$  to internal dissipated energy for any kinematically admissible deformation mode, considered as plastic only. In this study the upper bounds have been calculated by assuming a simple collapse mode containing a shear plane making an angle of  $45^\circ$  with the axis of symmetry. This collapse mechanism gives the best upper bounds for  $c/R < 1.59$ . For  $1.59 < c/R < 1.78$  the better upper bound on the yield load will be connected with the slip-line mechanism.

#### References

1. R. Hill, The plastic yielding of notched bars under tension, *Quart. J. Mech. Appl. Math.*, 2, 40 (1949).
2. J. F. W. Bishop, On the complete solution to problems of deformation of a plastic-rigid material, *J. Mech. Phys. Solids*, 2, 43 (1953).
3. R. Hill, The mathematical theory of plasticity, 2nd Ed., p.263, Oxford: Clarendon Press. 1956.
4. R. T. Shield, On the plastic flow of metals under conditions of axial symmetry, *Proc. Roy. Soc. A* 233, 267 (1955).
5. F. A. McClintock, On notch sensitivity, *Weld. J. Research suppl.*, May 1961.
6. W. Szczepiński, L. Dietrich, E. Drescher and J. Miastkowski, Plastic flow of axially-symmetric notched bars pulled in tension, *Int. J. Solids Struct.*, 2, 543 (1966).
7. G. Eason and R. T. Shield, The plastic indentation of a semi-infinite solid by a perfectly rough circular punch, *Zeits. Angew. Math. Phys.*, 11, 33 (1960).
8. R. Hill, The mathematical theory of plasticity, 2nd Ed., p.279, Oxford: Clarendon Press. 1956.
9. Z. Króć, Graphical solutions of axially-symmetric problems of plastic flow, *Zeits. Angew. Math. Phys.*, 18, 219 (1967).

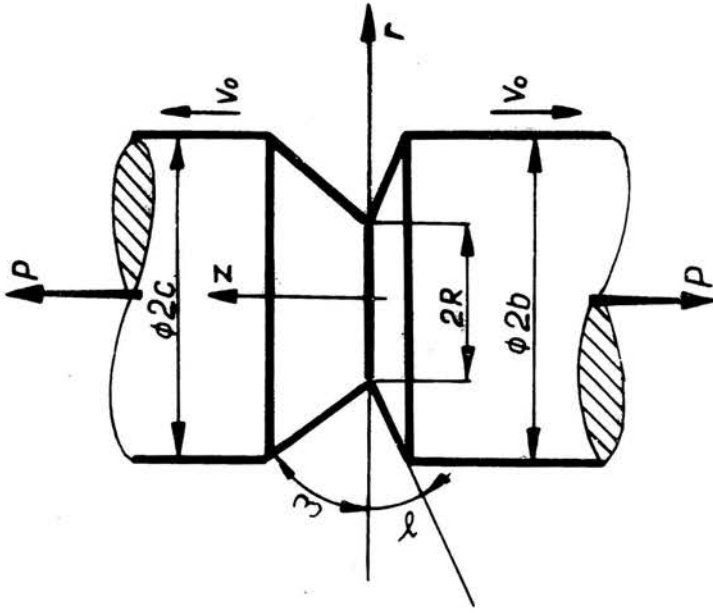


FIG. 2

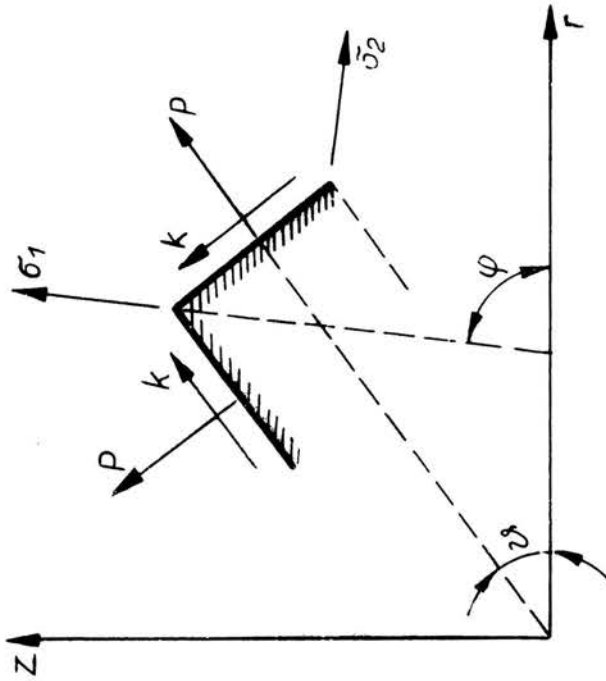
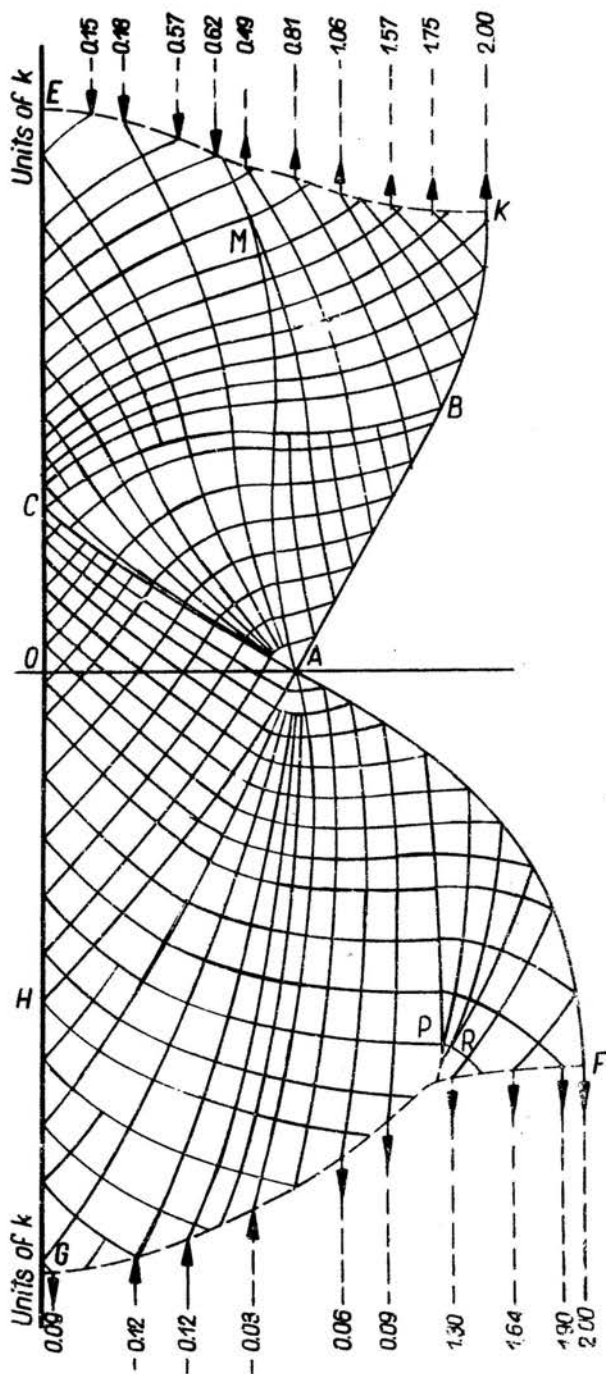
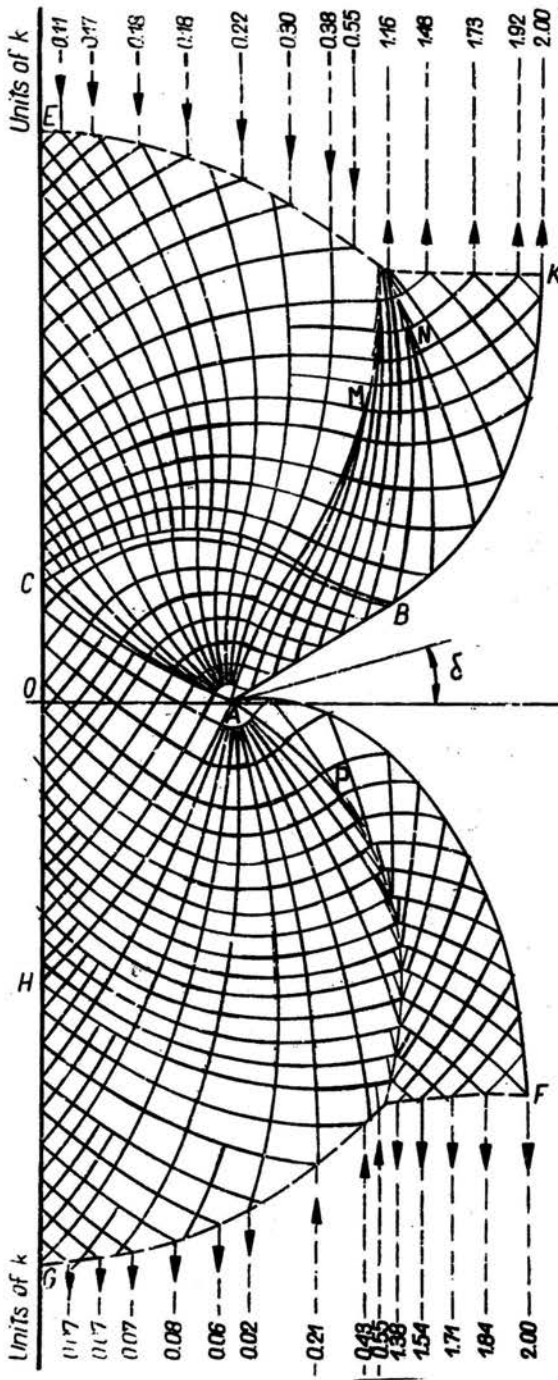


FIG. 1



**Fig. 3**



**Fig. 4**

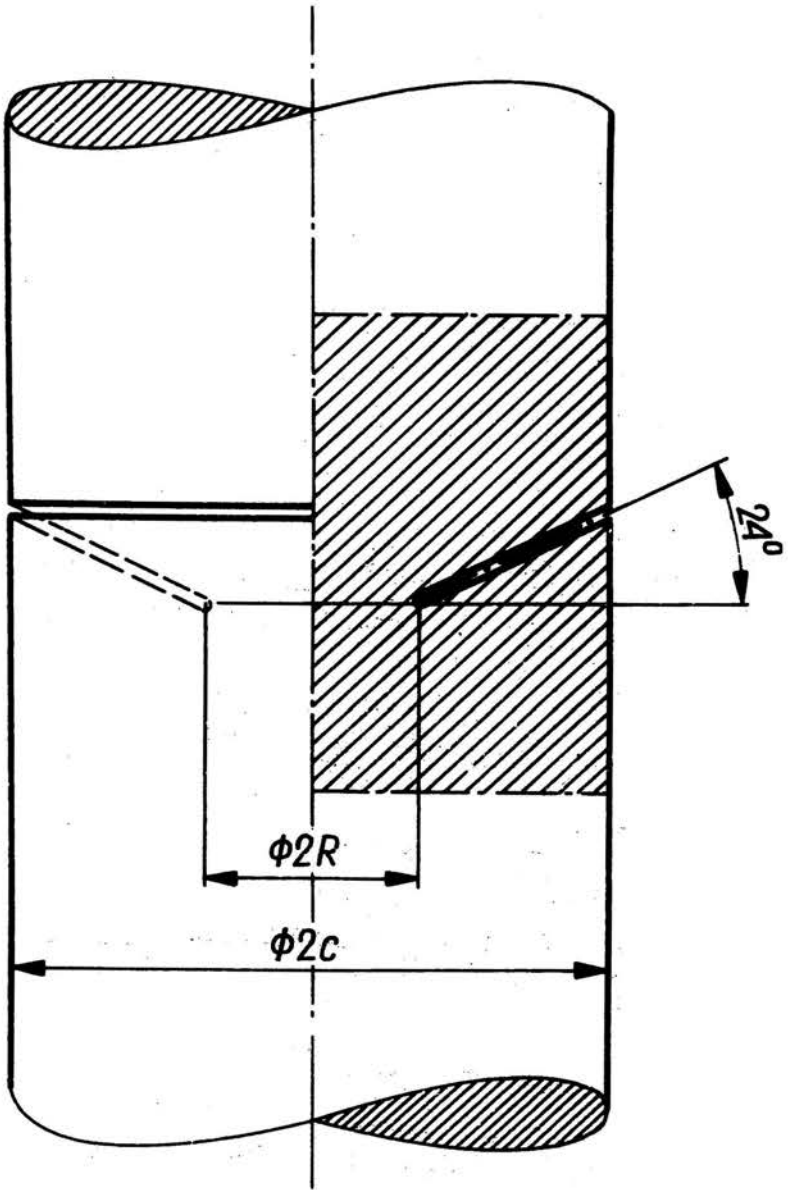


**Fig. 5**



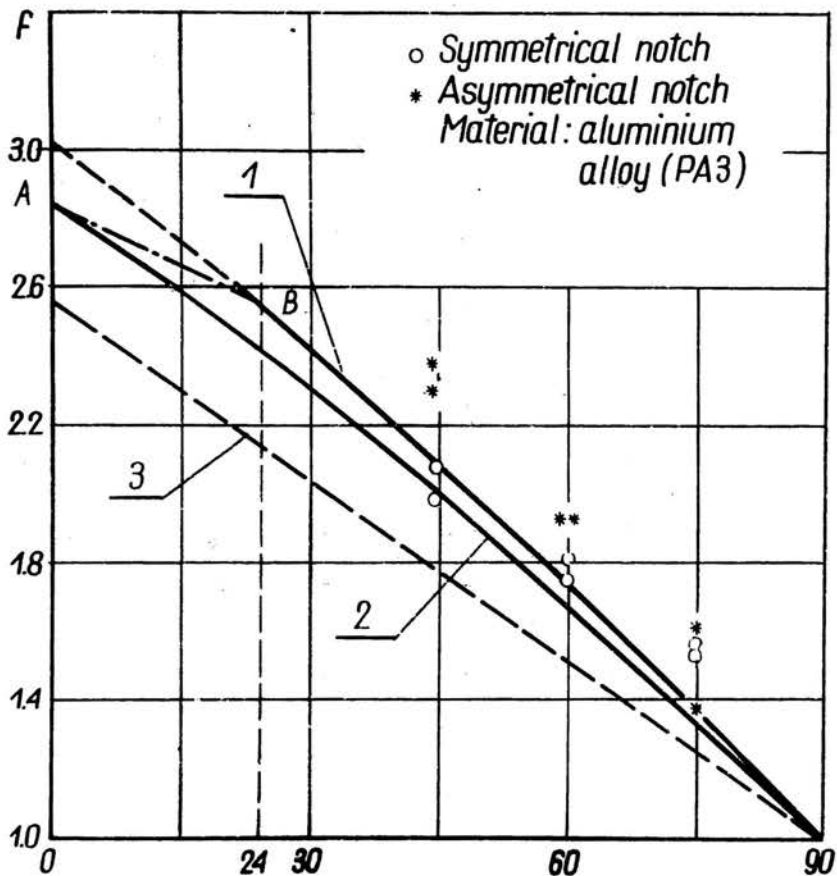


Fig. 6

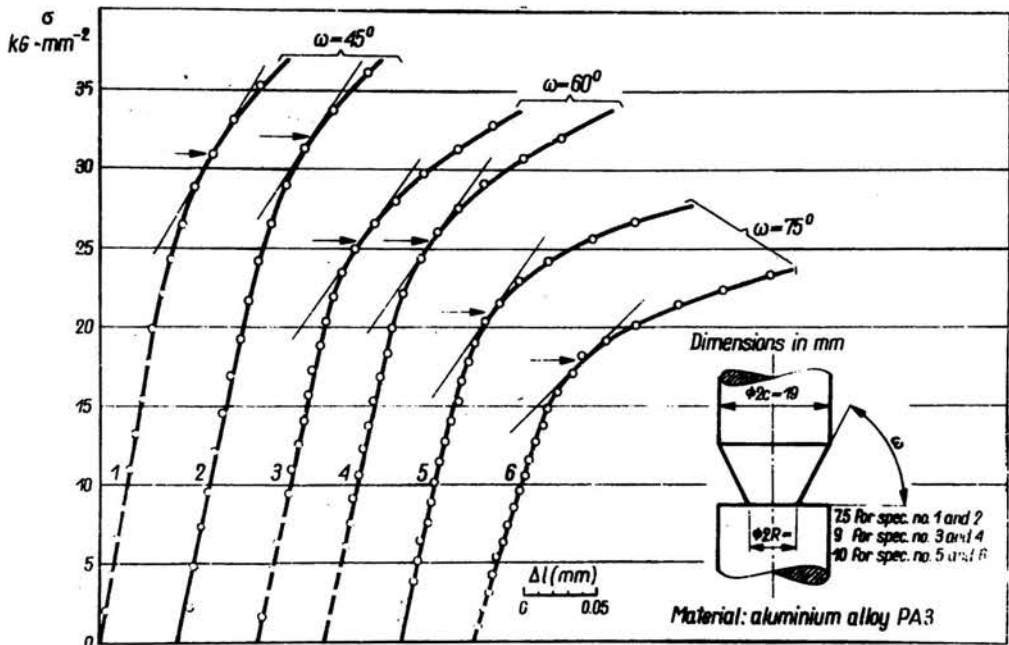


Fig. 7

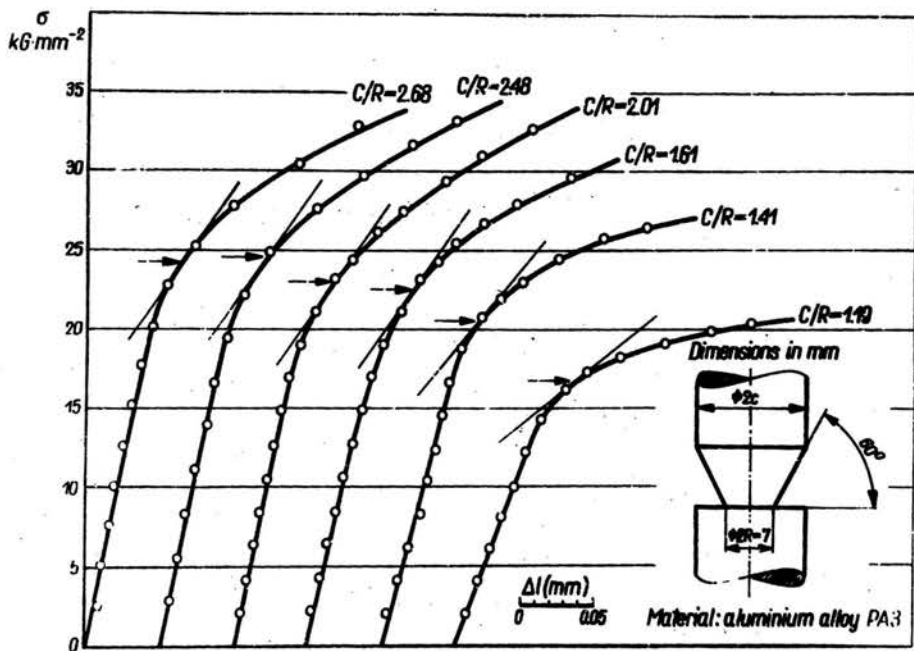


Fig. 8

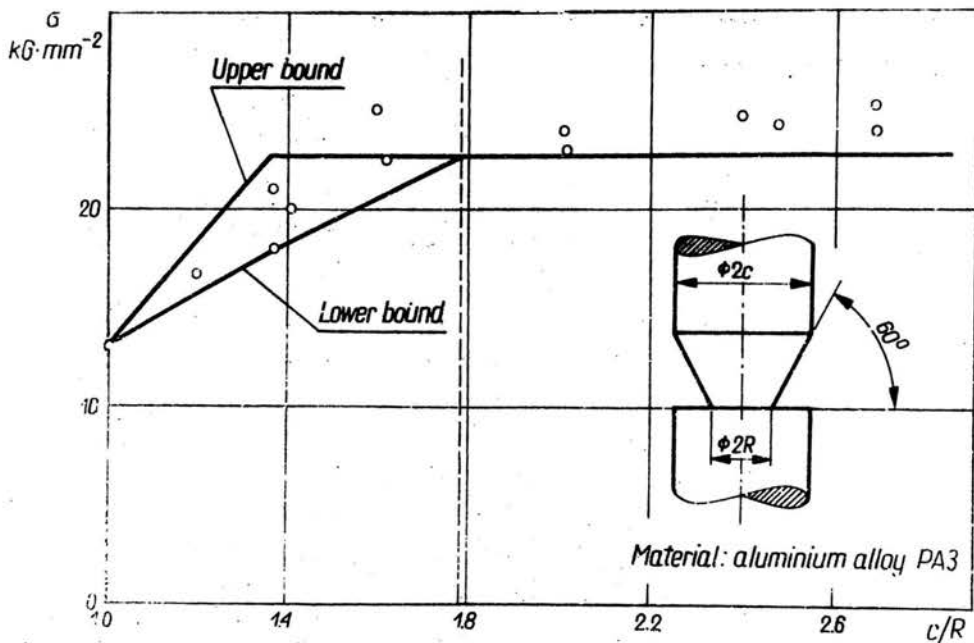
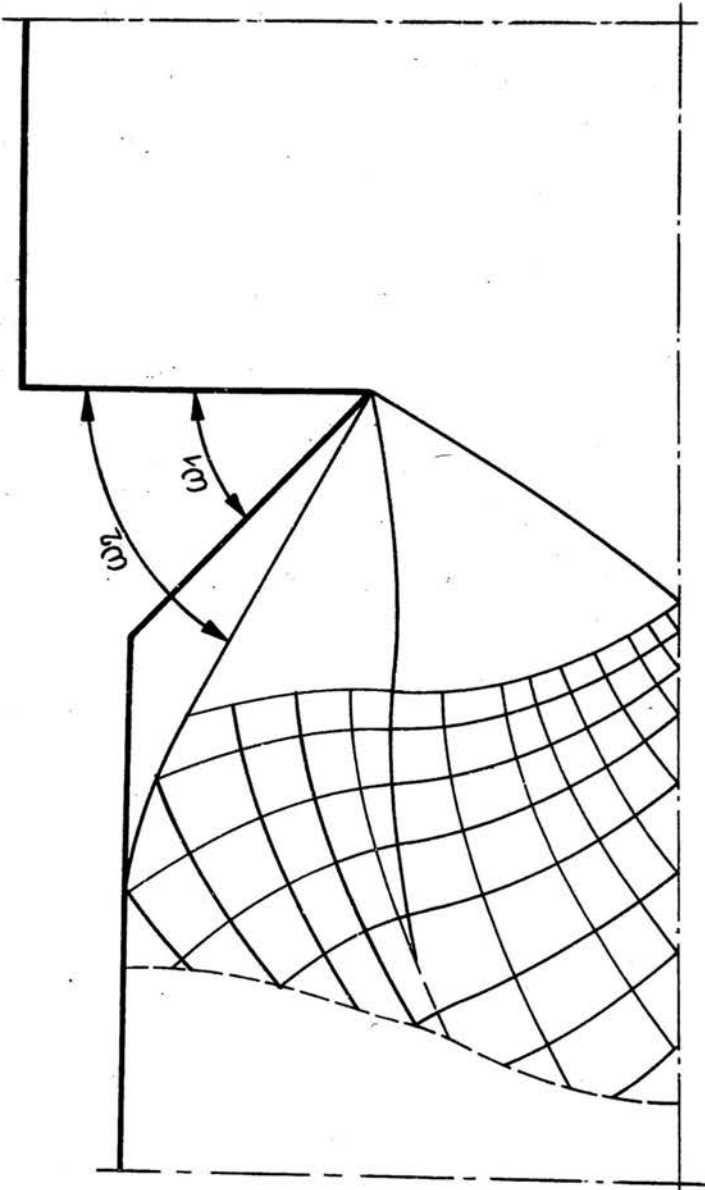


Fig. 9



**Fig. 10**